

# Primordial black holes and secondary gravitational waves from k/G inflation

Jiong Lin,<sup>1,\*</sup> Qing Gao,<sup>2,†</sup> Yungui Gong,<sup>1,‡</sup> Yizhou Lu,<sup>1,§</sup> Chao Zhang,<sup>1,¶</sup> and Fengge Zhang<sup>1,\*\*</sup>

<sup>1</sup>*School of Physics, Huazhong University of Science and Technology, Wuhan, Hubei 430074, China*

<sup>2</sup>*School of Physical Science and Technology, Southwest University, Chongqing 400715, China*

The possibility that in the mass range around  $10^{-12} M_\odot$  most of dark matter constitutes of primordial black holes (PBHs) is a very interesting topic. To produce PBHs with this mass, the primordial scalar power spectrum needs to be enhanced to the order of 0.01 at the scale  $k \sim 10^{12} \text{ Mpc}^{-1}$ . The enhanced power spectrum also produces large secondary gravitational waves at the mHz band. A phenomenological delta function power spectrum is usually used to discuss the production of PBHs and secondary gravitational waves. Based on G and k inflations, we propose a new mechanism to enhance the power spectrum at small scales by introducing a non-canonical kinetic term  $[1 - 2G(\phi)]X$  with the function  $G(\phi)$  having a peak. Away from the peak,  $G(\phi)$  is negligible and we recover the usual slow-roll inflation which is constrained by the cosmic microwave background anisotropy observations. Around the peak, the slow-roll inflation transiently turns to ultra slow-roll inflation. The enhancement of the power spectrum can be obtained with generic potentials, and there is no need to fine tune the parameters in  $G(\phi)$ . The energy spectrum  $\Omega_{GW}(f)$  of secondary gravitational waves have the characteristic power law behaviour  $\Omega_{GW}(f) \sim f^n$  and is testable by pulsar timing array and space based gravitational wave detectors.

*Introduction.*— The overdense inhomogeneities in the very early universe could gravitationally collapse to form primordial black holes (PBHs) [1, 2]. PBHs could have a vast range of masses in contrast to the black hole (BH) formed from the stellar evolution process, and they were used to explain the BH binary detected by LIGO and Virgo Collaboration [3–6]. Due to the failure of direct detection of particle dark matter (DM), it is warranted to consider the possibility of PBHs as DM candidate [7–15]. While light PBHs with mass  $M < 10^{15} g$  have been evaporated by now through the Hawking radiation [16], the mass window for PBHs as DM was strongly constrained by observations [17–32].

The production mechanism of PBHs could be the direct collapse of primordial curvature perturbations generated during inflation after horizon reentry. The amplitude of the primordial curvature perturbation at large scales is constrained by the cosmic microwave background (CMB) anisotropy measurements to be  $A_s = 2.1 \times 10^{-9}$  at the pivot scale  $k_* = 0.05 \text{ Mpc}^{-1}$  [33], and the formation of PBHs requires the amplitude of the primordial curvature perturbations  $A_s \sim \mathcal{O}(0.01)$ . Hence the enhancement of the amplitude should happen at small scales and this may be achieved by a field with inflection point [34–36]. Near the inflection point, the velocity of the inflaton dramatically decreases and the amplitude of the curvature perturbation is enhanced [37–45]. The production of PBHs by the enhanced primordial curvature perturbation is accompanied by the generation of secondary gravitational waves (GWs) [46–59]. There are other mechanisms to generate PBHs and GWs at the early universe [60–71]. However, it is a challenge to fine tune the model parameters to enhance the amplitude of the primordial curvature perturbation to the order of  $\mathcal{O}(0.01)$  while keeping the total number of e-folds to be  $N \simeq 50 - 60$  [72, 73]. A phenomenological delta function

power spectrum is usually used to discuss the production of PBHs and secondary GWs [51, 74, 75]. In this paper, based on the k inflation [76, 77] and G inflation [78–81], we propose a new mechanism to achieve the order  $\mathcal{O}(0.01)$  power spectrum at small scales by introducing a non-canonical kinetic term  $[1 - 2G(\phi)]X$  with the function  $G(\phi)$  having a peak at  $\phi_r$ . The productions of PBHs and secondary GWs are also discussed.

*k/G inflation.*— The action for G inflation is [78]

$$S = \int d^4x \sqrt{-g} \left[ \frac{1}{2} R + K(\phi, X) - G_3(\phi, X) \square \phi \right]. \quad (1)$$

where  $X = -g_{\mu\nu} \nabla^\mu \phi \nabla^\nu \phi / 2$ ,  $K$  and  $G_3$  are general functions of  $\phi$  and  $X$ . Assuming that the function  $G_3$  depends on  $\phi$  only, we can turn the term  $G_3(\phi) \square \phi$  to be  $-2G_{3\phi} X$  by partial integration, where  $G_{3\phi} = dG_3(\phi)/d\phi$ . Taking the function  $K(\phi, X) = X - V(\phi)$ , then the G inflation model becomes a k inflation model [76, 77],

$$\mathcal{L}_\phi = X - 2G(\phi)X - V(\phi), \quad (2)$$

where  $G(\phi) = G_{3\phi}$ . By assuming a spatially flat Friedmann-Walker (FRW) metric and a homogeneous scalar field  $\phi = \phi(t)$ , and varying the action (1), we get the Friedmann equation and Klein-Gordon equation

$$3H^2 = \frac{1}{2} \dot{\phi}^2 + V(\phi) - \dot{\phi}^2 G(\phi), \quad (3)$$

$$2\dot{H} + 3H^2 + \frac{1}{2} \dot{\phi}^2 - V(\phi) - \dot{\phi}^2 G(\phi) = 0, \quad (4)$$

$$\ddot{\phi} + 3H\dot{\phi} + \frac{V_\phi - \dot{\phi}^2 G_\phi}{1 - 2G(\phi)} = 0, \quad (5)$$

where  $G_\phi = dG(\phi)/d\phi$ . We define the slow-roll parameters

$$\epsilon_1 = -\frac{\dot{H}}{H^2}, \quad \epsilon_2 = -\frac{\ddot{\phi}}{H\dot{\phi}}, \quad \epsilon_3 = \frac{GX}{H^2}, \quad \epsilon_4 = \frac{G_\phi \dot{\phi}^2}{V_\phi}, \quad (6)$$

so slow-roll inflation is realized when  $|\epsilon_i| \ll 1$ , where  $i = 1, 2, 3, 4$ . By using Eqs. (3) and (4), the first slow-roll parameter  $\epsilon_1$  can be expressed as

$$\epsilon_1 = \frac{X(1-2G)}{H^2}. \quad (7)$$

To the first order of approximation, the quadratic action for the curvature perturbation  $\zeta$  is [77, 78],

$$S^{(2)} = \frac{1}{2} \int d\tau d^3x \tilde{z}^2 [\mathcal{G}(\zeta')^2 - \mathcal{F}(\vec{\nabla}\zeta)^2], \quad (8)$$

where  $\tilde{z} = \frac{a\dot{\phi}}{H}$ ,  $\mathcal{F} = \mathcal{G} = 1 - 2G$ , and the prime represents derivative with respect to the conformal time  $\tau$ . Since the sound speed for the scalar mode is  $c_s^2 = \mathcal{F}/\mathcal{G} = 1$ , so there is no problem with ghost and gradient instabilities. The scalar power spectrum is

$$P_\zeta = \frac{H^4}{4\pi^2 \dot{\phi}^2 (1-2G)} \simeq \frac{V^3}{12\pi^2 V_\phi^2} (1-2G), \quad (9)$$

and the scalar spectral index is

$$n_s - 1 = \frac{1}{1-2G} \left( 2\eta_V - 6\epsilon_V + \frac{2G_\phi}{1-2G} \sqrt{2\epsilon_V} \right), \quad (10)$$

where  $\epsilon_V = (V'/V)^2/2$  and  $\eta_V = V''/V$ . The scalar field does not affect the tensor perturbation, so the tensor power spectrum is [77, 78]

$$P_T = \frac{H^2}{2\pi^2}, \quad (11)$$

and the tensor to scalar ratio reads

$$r = \frac{P_T}{P_\zeta} = \frac{16X(1-2G)}{H^2} = 16\epsilon_1. \quad (12)$$

From the expression (9) for the scalar power spectrum, it is easy to get the enhancement of the power spectrum if the function  $G(\phi)$  has a peak. To be specific, we choose

$$-2G(\phi) = \frac{d}{\sqrt{\left(\frac{\phi-\phi_r}{c}\right)^2 + 1}}, \quad (13)$$

where the parameters  $\phi_r$  and  $c$  have the dimension of mass,  $c$  controls the width of the peak and the dimensionless parameter  $d$  determines the height of the peak. To get the enhancement over seven orders of magnitude,  $d$  is in the order of  $10^8$ . The number of e-folds around the peak is

$$\Delta N = \int_{\phi_r - \Delta\phi}^{\phi_r + \Delta\phi} \frac{H}{\dot{\phi}} d\phi \simeq - \int_{\phi_r - \Delta\phi}^{\phi_r + \Delta\phi} \frac{V(1-2G)}{V_\phi} d\phi. \quad (14)$$

Apparently, the number of e-folds around the peak can be very large. To keep the total number of e-folds before the end of inflation to be  $N \simeq 50 \sim 60$ , the peak width  $c$  should be small.

Due to the peak in  $G(\phi)$ , we may worry about the exit of inflation around  $\phi_r$  because of Eq. (7). However, Eq. (5) tells us that around the peak  $\epsilon_2 \approx 3$  and  $\dot{\phi}$  decreases dramatically. Therefore, it behaves like ultra slow-roll inflation [82–84] around  $\phi_r$ . When inflaton rolls close to  $\phi_r$ ,  $\dot{\phi}^2 G_\phi$  decreases and  $V_\phi$  gradually dominates over  $\dot{\phi}^2 G_\phi$ , so  $\epsilon_2$  decreases. When the inflaton rolls into the regime where  $\dot{\phi}^2 G_\phi < 0$  and  $\epsilon_2 < 0$ ,  $\dot{\phi}$  gradually increases toward the end of the inflation.

Because of the violation of slow-roll conditions, the expression (9) for the scalar power spectrum may not be applied and the enhancement of the power spectrum may not be reached. Let us exam how the power spectrum could be enhanced without using the formulae (9). The Fourier component of the curvature perturbation satisfies

$$\zeta_k'' + 2\frac{z'}{z}\zeta_k' + k^2\zeta_k = 0, \quad (15)$$

where  $z = (1-2G)^{1/2}\tilde{z}$  and

$$\frac{z'}{z} = aH \left[ 1 + \epsilon_1 - \epsilon_2 - \frac{G_\phi \dot{\phi}}{H(1-2G)} \right]. \quad (16)$$

When the velocity of the scalar field dramatically decreases and  $\epsilon_2 > 3$ , the friction term in Eq. (15) transiently changes sign, i.e.,  $z'/z < 0$ , as shown in Fig. 1. The friction term becomes a driving term and hence the curvature perturbation  $\zeta_k$  increases and the power spectrum is enhanced in this regime.

To show how the model and the above enhancement mechanism work, we consider the power law potential  $V(\phi) = \lambda\phi^p$  as examples. To be consistent with the observational constraint by CMB measurements [33], we choose  $p = 2/5$  and  $\lambda = 7.2 \times 10^{-10}$ . At the CMB scale  $k_* = 0.05 \text{ Mpc}^{-1}$  when the mode exits the horizon, the field value is  $\phi_* = 5.21$ , the scalar spectral tilt  $n_s \simeq 0.97$ , the tensor to scalar ratio  $r \simeq 0.045$ , the amplitude of the power spectrum is  $A_s \simeq 2.1 \times 10^{-9}$  and the number of e-folds before the end of inflation is  $N \simeq 54$ .

To get large enhancement  $O(0.01)$  at small scales, we choose the parameters in function  $G(\phi)$  as listed in Table I. As shown in Table I, the enhancement scale is adjusted by the parameter  $\phi_r$ . If  $\phi_r$  is further away from  $\phi_*$ , then the enhancement scale becomes smaller. As discussed above, the peak in  $G(\phi)$  violates the slow-roll condition, so we numerically solve Eq. (15) to obtain the power spectrum and the corresponding values at the peak scales are shown in Table I.

In Fig. 1 we plot the evolutions of  $\phi$ ,  $\epsilon_1$ ,  $\epsilon_2$  and  $z'/(zaH)$  with the parameter set C. We see that around  $N \sim 30$  the inflaton rolls very slowly and its velocity decreases to be very small, so the slow-roll parameter  $\epsilon_1$  becomes negligible which enhances the power spectrum dramatically. Note that the slow-roll parameter  $\epsilon_2$  becomes very large and changes quickly, the term  $-2G(\phi)X$

TABLE I. The chosen parameter sets and the results for the scalar power spectrum and PBH abundances at small peak scales.

Sets	$\phi_r$	$d$	$c$	$k_{\text{peak}}/\text{Mpc}^{-1}$	$P_{\zeta(\text{peak})}$	$M_{\text{pbh}}^{\text{peak}}/M_{\odot}$	$f_{\text{PBH}}^{\text{peak}}$
A	4.5	$5.26 \times 10^8$	$9.54 \times 10^{-11}$	$2.97 \times 10^5$	$1.88 \times 10^{-2}$	26.8	0.00148
B	4.1	$5.26 \times 10^8$	$1.05 \times 10^{-10}$	$3.16 \times 10^7$	$1.7 \times 10^{-2}$	$2 \times 10^{-3}$	0.0167
C	2.97	$5.26 \times 10^8$	$1.4658 \times 10^{-10}$	$1.36 \times 10^{12}$	$1.33 \times 10^{-2}$	$1.28 \times 10^{-12}$	0.85
D	2.97	$5.26 \times 10^8$	$1.461 \times 10^{-10}$	$1.35 \times 10^{12}$	$1.15 \times 10^{-2}$	$1.3 \times 10^{-12}$	0.006

effectively flattens the potential and makes it behave like ultra-roll inflation.

In Fig. 2, we show the results for the scalar power spectrum. At large scales, the power spectrum is in the order of  $\mathcal{O}(10^{-9})$ , which is compatible with CMB constraints [33]. At small scales, the power spectrum is enhanced to the order of  $\mathcal{O}(0.01)$ , which is large enough to produce PBHs after the horizon reentry as discussed below. The models also satisfy the constraints from CMB  $\mu$ -distortion, big bang nucleosynthesis (BBN) and pulsar timing array (PTA) observations [85–87].

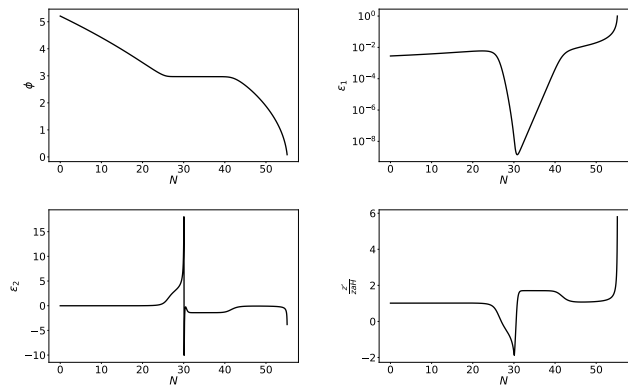


FIG. 1. The evolution of  $\phi$ ,  $\epsilon_1$ ,  $\epsilon_2$  and  $z'/(zaH)$  with the parameter set C. We take the number of e-folds  $N$  before the end of inflation as the time.

*PBH production.*— When the primordial curvature perturbation reenters the horizon during radiation dominated era, it may gravitationally collapse to form PBHs. The PBH mass is equal to  $\gamma M_{\text{hor}}$ , where  $M_{\text{hor}}$  is the horizon mass and we choose the factor  $\gamma = 0.2$  [88]. The current fractional energy density of PBHs with mass  $M$  to DM is [12, 36]

$$f_{\text{PBH}}(M) = \frac{\beta(M)}{3.94 \times 10^{-9}} \left(\frac{\gamma}{0.2}\right)^{1/2} \left(\frac{g_*}{10.75}\right)^{-1/4} \times \left(\frac{0.12}{\Omega_{\text{DM}} h^2}\right) \left(\frac{M}{M_{\odot}}\right)^{-1/2}, \quad (17)$$

where  $M_{\odot}$  is the solar mass,  $g_*$  is the effective degrees of freedom at the formation time,  $\Omega_{\text{DM}}$  is the current energy density parameter of DM, the fractional energy density

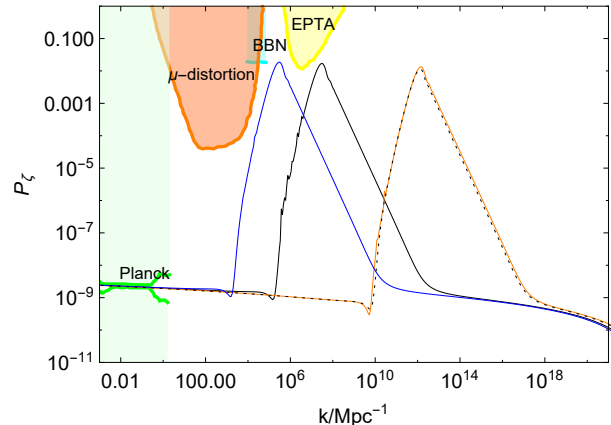


FIG. 2. The results for the scalar power spectrum. The blue line uses the parameter set A, the solid black line uses the parameter set B, the orange line uses the parameter set C, and the dotted black line uses the parameter set D. The lightgreen shaded region is excluded by the CMB observations [33]. The yellow, cyan and orange regions show the constraints from the PTA observations [85], the effect on the ratio between neutron and proton during the big bang nucleosynthesis (BBN) [86] and  $\mu$ -distortion of CMB [87], respectively.

of PBHs at the formation is [89–91]

$$\beta(M) = \sqrt{\frac{2}{\pi}} \frac{\sigma(M)}{\delta_c} \exp\left(-\frac{\delta_c^2}{2\sigma^2(M)}\right), \quad (18)$$

$\delta_c$  is the critical density perturbation for the PBH formation,  $\sigma(k)$  is the mass variance associated with the PBH mass  $M(k)$  smoothing on the comoving horizon length  $k^{-1} = 1/(aH)$  [89, 90]

$$\sigma^2(k) = \left(\frac{4}{9}\right)^2 \int \frac{dq}{q} W^2(q/k) (q/k)^4 P_{\zeta}(q), \quad (19)$$

and the Gaussian window function  $W(x) = \exp(-x^2/2)$ . The effective degrees of freedom  $g_* = 107.5$  for  $T > 300\text{GeV}$  and  $g_* = 10.75$  for  $0.5\text{MeV} < T < 300\text{GeV}$ . We take the observational value  $\Omega_{\text{DM}} h^2 = 0.12$  [92] and  $\delta_c = 0.4$  [91, 93, 94] for the calculation of PBH abundance. The relation between the PBH mass  $M$  and the scale  $k$  is [36]

$$M(k) = 3.68 \left(\frac{\gamma}{0.2}\right) \left(\frac{g_*}{10.75}\right)^{-1/6} \left(\frac{k}{10^6 \text{ Mpc}^{-1}}\right)^{-2} M_{\odot}. \quad (20)$$

With the approximation that the power spectrum is scale invariant, we get  $\sigma(k) \simeq (4/9)\sqrt{P_\zeta}$ , and

$$\beta(M) \approx \sqrt{\frac{2}{\pi}} \frac{\sqrt{P_\zeta}}{\mu_c} \exp\left(-\frac{\mu_c^2}{2P_\zeta}\right),$$

where  $\mu_c = 9\delta_c/4$ .

Substituting the obtained power spectrum into Eqs. (17), (18), (19) and (20), we get the PBH abundances as shown in Table I and Fig. 3. For the parameter set A, the model produces PBHs with mass  $M \simeq 27M_\odot$  and abundance  $f \simeq 1.48 \times 10^{-3}$ , which may explain the BBH event GW150914 observed by LIGO [3]. In this mass range PBHs cannot consist of all DM due to the constraints from CMB [27]. For the parameter set B, the model produces PBHs with mass  $M \simeq 2 \times 10^{-3}M_\odot$  and abundance  $f \simeq 0.017$ . For the parameter sets C and D, the model produces PBHs with mass  $M \simeq 10^{-12}M_\odot$ . The produced PBH abundance is  $f \simeq 0.85$  for the parameter set C and  $f \simeq 6 \times 10^{-3}$  for the parameter set D. In this mass range, the observational constraint on PBH abundances are absent [95], so all DM can be PBHs.

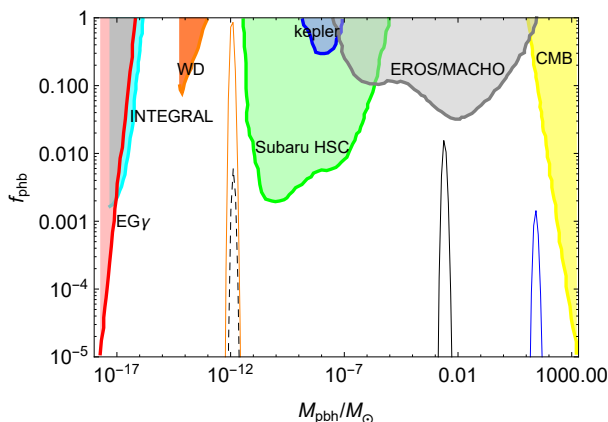


FIG. 3. The PBH abundances for the parameter sets A (the blue line), B (the black solid line), C (the brown line) and D (the black dashed line). The shaded regions show the observational constraints on the PBH abundance: the yellow region from accretion constraints by CMB [27], the red region from extragalactic gamma-rays by PBH evaporation ( $EG\gamma$ ) [23], the cyan region from galactic center 511 keV gamma-ray line (INTEGRAL) [31], the orange region from white dwarf explosion (WD) [26], the green region from microlensing events with Subaru HSC (Subaru HSC)[30], the blue region from the Kepler satellite [24], the gray region from the EROS/MACHO [22].

*Secondary GWs.*— In addition to the production of PBHs, the large density perturbations generated at small scales during inflation could produce secondary GWs and be tested by the future PTA observations and space based GW observatory. The Fourier components of the second order tensor perturbations  $h_{\mathbf{k}}$  satisfy [48, 49]

$$h''_{\mathbf{k}} + 2\mathcal{H}h'_{\mathbf{k}} + k^2 h_{\mathbf{k}} = 4S_{\mathbf{k}}, \quad (21)$$

with the source

$$S_{\mathbf{k}} = \int \frac{d^3\tilde{\mathbf{k}}}{(2\pi)^{3/2}} e_{ij}(\mathbf{k}) \tilde{k}^i \tilde{k}^j \left[ 2\Phi_{\tilde{\mathbf{k}}}\Phi_{\mathbf{k}-\tilde{\mathbf{k}}} + \frac{4}{3(1+\omega)\mathcal{H}^2} \times (\Phi'_{\tilde{\mathbf{k}}} + \mathcal{H}\Phi_{\tilde{\mathbf{k}}}) (\Phi'_{\mathbf{k}-\tilde{\mathbf{k}}} + \mathcal{H}\Phi_{\mathbf{k}-\tilde{\mathbf{k}}}) \right], \quad (22)$$

where  $\mathcal{H} = aH$ ,  $\omega = p/\rho$ ,  $e_{ij}(\mathbf{k})$  is the polarization tensor, the Bardeen potential  $\Phi_{\mathbf{k}} = \Psi(k\eta)\phi_{\mathbf{k}}$ , the transfer function  $\Psi$  in the radiation domination is

$$\Psi(x) = \frac{9}{x^2} \left( \frac{\sin(x/\sqrt{3})}{x/\sqrt{3}} - \cos(x/\sqrt{3}) \right), \quad (23)$$

and the primordial value  $\phi_{\mathbf{k}}$  is

$$\langle \phi_{\mathbf{k}}\phi_{\tilde{\mathbf{k}}} \rangle = \delta^{(3)}(\mathbf{k} + \tilde{\mathbf{k}}) \frac{2\pi^2}{k^3} \left( \frac{3+3w}{5+3w} \right)^2 P_\zeta(k), \quad (24)$$

Solving Eq. (21) by using the Green function method, we obtain the energy density of induced GWs generated in the radiation domination [44, 58, 96, 97]

$$\Omega_{GW}(k, \eta) = \frac{1}{6} \left( \frac{k}{aH} \right)^2 \int_0^\infty dv \int_{|1-v|}^{1+v} du \left\{ \left[ \frac{4v^2 - (1-u^2+v^2)^2}{4uv} \right]^2 \times \overline{I_{RD}^2}(u, v, x \rightarrow \infty) P_\zeta(kv) P_\zeta(ku) \right\}, \quad (25)$$

where  $u = |\mathbf{k} - \tilde{\mathbf{k}}|/k$ ,  $v = \tilde{k}/k$ ,  $x = k\eta$  and  $\overline{I_{RD}^2}$  is the oscillation time average. The integral kernel  $I_{RD}$  is [44, 97]

$$I_{RD} = \int_1^x dy y \sin(x-y) \{ 3\Psi(uy)\Psi(vy) + y[\Psi(vy)u\Psi'(uy) + v\Psi'(vy)\Psi(uy)] + y^2 uv\Psi'(uy)\Psi'(vy) \}, \quad (26)$$

and an analytical expression for  $I_{RD}$  was given in Refs. [44, 97]. Plugging the power spectrum in Fig. 2 into Eq. (25) and using Eqs. (23) and (26) we obtain the induced GWs and the results are shown in Fig. 4. If we use the analytical expression for  $I_{RD}$  in Ref. [96], the difference on the secondary GWs is small for the power spectrum discussed in this paper. To compare the results with observations, in Fig. 4, we also show the sensitivity curves for European PTA (EPTA) [98–101], the Square Kilometer Array (SKA) [102], Advanced Laser Interferometer Gravitational Wave Observatory (aLIGO) [103, 104], Laser Interferometer Space Antenna (LISA) [105, 106], TaiJi [107] and TianQin [108].

As shown in Fig. 4, for the parameter sets C and D, the induced GWs are in the mHz band and could be tested by the future space based detector like LISA, TaiJi

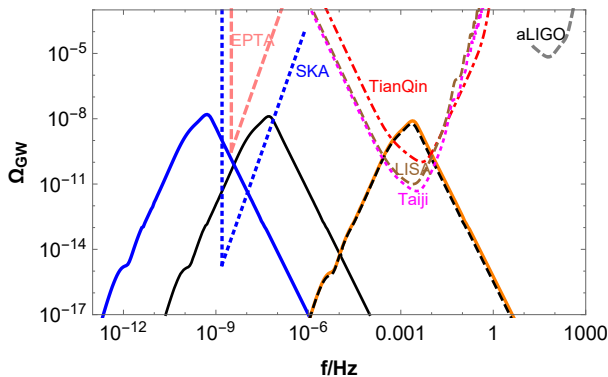


FIG. 4. The secondary GWs generated in the model. The solid blue, solid black, solid orange and dashed black lines denote the results for the model parameter sets A, B, C and D, respectively. The pink dashed curve denotes the EPTA limit [98–101], the blue dotted curve denotes the SKA limit [102], the red dot-dashed curve in the middle denotes the TianQin limit [108], the dotted magenta curve shows the TaiJi limit [107], the brown dashed curve shows the LISA limit [106], and the gray dotted curve denotes the aLIGO limit [103, 104].

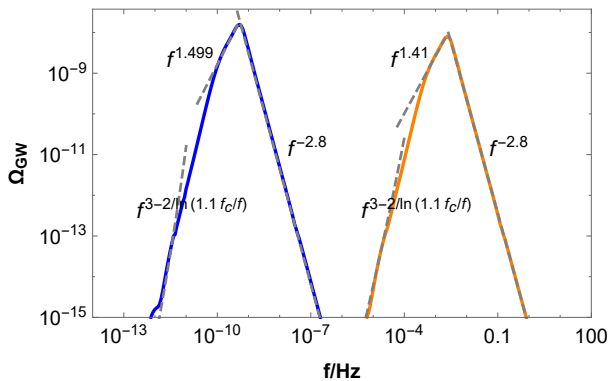


FIG. 5. The power law behaviours for the energy spectra of secondary GWs. The solid blue and orange lines denote the energy spectra for the parameter sets A and C, respectively.

and TianQin. The induced GWs from the parameter set A have the peak frequency  $f \sim 10^{-10}$  Hz and those from the parameter set B have the peak frequency  $f \sim 10^{-7}$  Hz, both of them could be tested by SKA. Taking 4 years’ observational time, the signal to noise ratio [109] for induced GWS from the parameter set C in LISA is  $\text{SNR} = 34655$ ,  $\text{SNR} = 66359$  in Taiji and  $\text{SNR} = 2496$  in TianQin.

It is interesting to note that the energy spectrum of secondary GWs around the peak frequency can be parameterized as the power law form  $\Omega_{GW}(f) \sim f^n$  [45, 67, 110], and the parametrization of stochastic GW background is a powerful tool in probing the cosmic history [111]. As shown in Fig. 5, for the parameter set A,  $\Omega_{GW} \sim f^{1.499}$  for  $f < f_c = 4.4 \times 10^{-10}$  Hz and  $\Omega_{GW} \sim f^{-2.8}$  for  $f > f_c$ . For the parameter set C,  $\Omega_{GW} \sim f^{1.41}$  for

$f < f_c = 2.5 \times 10^{-3}$  Hz and  $\Omega_{GW} \sim f^{-2.8}$  for  $f > f_c$ . In the regions with  $f \ll f_c$ , the log dependent power index [110] is  $n = 3 - 2/\ln(1.1f_c/f)$ .

*Conclusion.*— It is possible that most of DM constitutes of PBHs if the mass of PBH DM is in the order of  $10^{-12} M_\odot$ . To produce the order one  $f_{\text{PBH}}$  with this mass, the curvature power spectrum needs to be in the order of 0.01 at the scale  $k \sim 10^{12} \text{ Mpc}^{-1}$ . This large power spectrum also generates large secondary GWs at the mHz band which can be observed by the future space based GW observatory like LISA, TaiJi and TianQin. However, it is difficult to enhance the power spectrum for a single canonical field inflation. By considering non-canonical inflation like G or k inflation, we find a new mechanism to produce PBH DM and secondary GWs. In particular, the field dependent kinetic term  $[1 - 2G(\phi)]X$  can arise from G inflation or k inflation, and we propose that the function  $G(\phi)$  has a peak at  $\phi_r$ . The power spectrum is enhanced around the peak, the PBH mass and the frequency of secondary GWs are determined by the value of  $\phi_r$ . Away from the peak,  $G(\phi)$  is negligible and we recover the usual slow-roll inflation which is constrained by the CMB observations. Around the peak, the potential becomes effectively a flat plateau and the slow-roll inflation transiently turns to ultra slow-roll inflation.

We use the power law potential as an example to produce non-negligible PBH abundances with masses around  $27M_\odot$ ,  $10^{-3}M_\odot$  and  $10^{-12}M_\odot$ , and secondary GWs with frequencies around 10nHz,  $10^{-7}$  Hz and mHz. The PBH DM with the stellar mass of  $27M_\odot$  could be the black holes observed by LIGO and Virgo collaboration. To enhance the power spectrum by seven orders of magnitude, the parameter  $d$  should be in the order of  $10^8$ . The parameter  $c$  is in the order of  $10^{-10}$  so that away from the peak the function  $G(\phi)$  is negligible and the usual slow-roll is guaranteed. We give four parameters sets to show how the enhancement of the power spectrum at different scales can be achieved. By changing the parameter  $c$  from  $1.4658 \times 10^{-10}$  to  $1.461 \times 10^{-10}$ , the PBH peak abundances decrease from  $f_{\text{PBH}} = 0.85$  to  $f_{\text{PBH}} = 0.006$ , so the model may accommodate more robust constraints on  $f_{\text{PBH}}$ . The secondary GWs generated by the model have the characteristic power law behaviour  $\Omega_{GW}(f) \sim f^n$  and are testable by either PTA or LISA/TaiJi/TianQin observations.

This research was supported in part by the National Natural Science Foundation of China under Grant No. 11875136 and the Major Program of the National Natural Science Foundation of China under Grant No. 11690021.

\* jionglin@hust.edu.cn

† gaoqing1024@swu.edu.cn

‡ Corresponding author. yggong@hust.edu.cn

- § louis chou@hust.edu.cn  
 ¶ chao zhang@hust.edu.cn  
 \*\* fenggezhang@hust.edu.cn
- [1] B. J. Carr and S. W. Hawking, *Mon. Not. Roy. Astron. Soc.* **168**, 399 (1974).
  - [2] S. Hawking, *Mon. Not. Roy. Astron. Soc.* **152**, 75 (1971).
  - [3] B. P. Abbott *et al.* (LIGO Scientific, Virgo), *Phys. Rev. Lett.* **116**, 061102 (2016), arXiv:1602.03837 [gr-qc].
  - [4] B. P. Abbott *et al.* (LIGO Scientific, Virgo), *Phys. Rev. Lett.* **116**, 241103 (2016), arXiv:1606.04855 [gr-qc].
  - [5] S. Bird, I. Cholis, J. B. Muñoz, Y. Ali-Haïmoud, M. Kamionkowski, E. D. Kovetz, A. Raccanelli, and A. G. Riess, *Phys. Rev. Lett.* **116**, 201301 (2016), arXiv:1603.00464 [astro-ph.CO].
  - [6] M. Sasaki, T. Suyama, T. Tanaka, and S. Yokoyama, *Phys. Rev. Lett.* **117**, 061101 (2016), [Erratum: *Phys. Rev. Lett.* **121**, no.5, 059901 (2018)], arXiv:1603.08338 [astro-ph.CO].
  - [7] P. Ivanov, P. Naselsky, and I. Novikov, *Phys. Rev. D* **50**, 7173 (1994).
  - [8] P. H. Frampton, M. Kawasaki, F. Takahashi, and T. T. Yanagida, *JCAP* **1004**, 023 (2010), arXiv:1001.2308 [hep-ph].
  - [9] K. M. Belotsky, A. D. Dmitriev, E. A. Esipova, V. A. Gani, A. V. Grobov, M. Yu. Khlopov, A. A. Kirillov, S. G. Rubin, and I. V. Svadkovsky, *Mod. Phys. Lett. A* **29**, 1440005 (2014), arXiv:1410.0203 [astro-ph.CO].
  - [10] M. Yu. Khlopov, S. G. Rubin, and A. S. Sakharov, *Astropart. Phys.* **23**, 265 (2005), arXiv:astro-ph/0401532 [astro-ph].
  - [11] S. Clesse and J. García-Bellido, *Phys. Rev. D* **92**, 023524 (2015), arXiv:1501.07565 [astro-ph.CO].
  - [12] B. Carr, F. Kuhnel, and M. Sandstad, *Phys. Rev. D* **94**, 083504 (2016), arXiv:1607.06077 [astro-ph.CO].
  - [13] K. Inomata, M. Kawasaki, K. Mukaida, Y. Tada, and T. T. Yanagida, *Phys. Rev. D* **96**, 043504 (2017), arXiv:1701.02544 [astro-ph.CO].
  - [14] J. García-Bellido, *Proceedings, 11th International LISA Symposium: Zurich, Switzerland, September 5-9, 2016*, *J. Phys. Conf. Ser.* **840**, 012032 (2017), arXiv:1702.08275 [astro-ph.CO].
  - [15] E. D. Kovetz, *Phys. Rev. Lett.* **119**, 131301 (2017), arXiv:1705.09182 [astro-ph.CO].
  - [16] S. W. Hawking, *Euclidean quantum gravity*, *Commun. Math. Phys.* **43**, 199 (1975), [167(1975)].
  - [17] A. Gould, *Astrophys. J. Lett.* **386**, L5 (1992).
  - [18] J. J. Dalcanton, C. R. Canizares, A. Granados, C. C. Steidel, and J. T. Stocke, *Astrophys. J.* **424**, 550 (1994).
  - [19] R. A. Allsman *et al.* (Macho), *Astrophys. J. Lett.* **550**, L169 (2001), arXiv:astro-ph/0011506 [astro-ph].
  - [20] R. J. Nemiroff, G. F. Marani, J. P. Norris, and J. T. Bonnell, *Phys. Rev. Lett.* **86**, 580 (2001), arXiv:astro-ph/0101488 [astro-ph].
  - [21] P. N. Wilkinson, D. R. Henstock, I. W. A. Browne, A. G. Polatidis, P. Augusto, A. C. S. Readhead, T. J. Pearson, W. Xu, G. B. Taylor, and R. C. Vermeulen, *Phys. Rev. Lett.* **86**, 584 (2001), arXiv:astro-ph/0101328 [astro-ph].
  - [22] P. Tisserand *et al.* (EROS-2), *Astron. Astrophys.* **469**, 387 (2007), arXiv:astro-ph/0607207 [astro-ph].
  - [23] B. J. Carr, K. Kohri, Y. Sendouda, and J. Yokoyama, *Phys. Rev. D* **81**, 104019 (2010), arXiv:0912.5297 [astro-ph.CO].
  - [24] K. Griest, A. M. Cieplak, and M. J. Lehner, *Phys. Rev. Lett.* **111**, 181302 (2013).
  - [25] D. M. Jacobs, G. D. Starkman, and B. W. Lynn, *Mon. Not. Roy. Astron. Soc.* **450**, 3418 (2015), arXiv:1410.2236 [astro-ph.CO].
  - [26] P. W. Graham, S. Rajendran, and J. Varela, *Phys. Rev. D* **92**, 063007 (2015), arXiv:1505.04444 [hep-ph].
  - [27] Y. Ali-Haïmoud and M. Kamionkowski, *Phys. Rev. D* **95**, 043534 (2017), arXiv:1612.05644 [astro-ph.CO].
  - [28] S. Wang, Y.-F. Wang, Q.-G. Huang, and T. G. F. Li, *Phys. Rev. Lett.* **120**, 191102 (2018), arXiv:1610.08725 [astro-ph.CO].
  - [29] B. Carr, M. Raidal, T. Tenkanen, V. Vaskonen, and H. Veermäe, *Phys. Rev. D* **96**, 023514 (2017), arXiv:1705.05567 [astro-ph.CO].
  - [30] H. Niikura *et al.*, *Nat. Astron.* **3**, 524 (2019), arXiv:1701.02151 [astro-ph.CO].
  - [31] R. Laha, (2019), arXiv:1906.09994 [astro-ph.HE].
  - [32] G. Sato-Polito, E. D. Kovetz, and M. Kamionkowski, *Phys. Rev. D* **100**, 063521 (2019), arXiv:1904.10971 [astro-ph.CO].
  - [33] Y. Akrami *et al.* (Planck), (2018), arXiv:1807.06211 [astro-ph.CO].
  - [34] C. Germani and T. Prokopec, *Phys. Dark Univ.* **18**, 6 (2017), arXiv:1706.04226 [astro-ph.CO].
  - [35] H. Motohashi and W. Hu, *Phys. Rev. D* **96**, 063503 (2017), arXiv:1706.06784 [astro-ph.CO].
  - [36] H. Di and Y. Gong, *JCAP* **1807**, 007 (2018), arXiv:1707.09578 [astro-ph.CO].
  - [37] K. Dimopoulos, *Phys. Lett. B* **775**, 262 (2017), arXiv:1707.05644 [hep-ph].
  - [38] J. Garcia-Bellido and E. Ruiz Morales, *Phys. Dark Univ.* **18**, 47 (2017), arXiv:1702.03901 [astro-ph.CO].
  - [39] M. Kawasaki, A. Kusenko, Y. Tada, and T. T. Yanagida, *Phys. Rev. D* **94**, 083523 (2016), arXiv:1606.07631 [astro-ph.CO].
  - [40] S.-L. Cheng, W. Lee, and K.-W. Ng, *Phys. Rev. D* **99**, 063524 (2019), arXiv:1811.10108 [astro-ph.CO].
  - [41] T.-J. Gao and Z.-K. Guo, *Phys. Rev. D* **98**, 063526 (2018), arXiv:1806.09320 [hep-ph].
  - [42] M. Cicoli, V. A. Diaz, and F. G. Pedro, *JCAP* **1806**, 034 (2018), arXiv:1803.02837 [hep-th].
  - [43] J. R. Espinosa, D. Racco, and A. Riotto, *Phys. Rev. Lett.* **120**, 121301 (2018), arXiv:1710.11196 [hep-ph].
  - [44] J. R. Espinosa, D. Racco, and A. Riotto, *JCAP* **1809**, 012 (2018), arXiv:1804.07732 [hep-ph].
  - [45] W.-T. Xu, J. Liu, T.-J. Gao, and Z.-K. Guo, *Phys. Rev. D* **101**, 023505 (2020), arXiv:1907.05213 [astro-ph.CO].
  - [46] S. Matarrese, S. Mollerach, and M. Bruni, *Phys. Rev. D* **58**, 043504 (1998), arXiv:astro-ph/9707278 [astro-ph].
  - [47] S. Mollerach, D. Harari, and S. Matarrese, *Phys. Rev. D* **69**, 063002 (2004), arXiv:astro-ph/0310711 [astro-ph].
  - [48] K. N. Ananda, C. Clarkson, and D. Wands, *Phys. Rev. D* **75**, 123518 (2007), arXiv:gr-qc/0612013 [gr-qc].
  - [49] D. Baumann, P. J. Steinhardt, K. Takahashi, and K. Ichiki, *Phys. Rev. D* **76**, 084019 (2007), arXiv:hep-th/0703290 [hep-th].
  - [50] J. Garcia-Bellido, M. Peloso, and C. Unal, *JCAP* **1709**, 013 (2017), arXiv:1707.02441 [astro-ph.CO].
  - [51] R. Saito and J. Yokoyama, *Phys. Rev. Lett.* **102**, 161101 (2009), [Erratum: *Phys. Rev. Lett.* **107**, 069901 (2011)], arXiv:0812.4339 [astro-ph].
  - [52] R. Saito and J. Yokoyama, *Prog. Theor. Phys.* **123**, 867 (2010), [Erratum: *Prog. Theor. Phys.* **126**, 351 (2011)], arXiv:0912.5317 [astro-ph.CO].

- [53] E. Bugaev and P. Klimai, Phys. Rev. D **81**, 023517 (2010), arXiv:0908.0664 [astro-ph.CO].
- [54] E. Bugaev and P. Klimai, Phys. Rev. D **83**, 083521 (2011), arXiv:1012.4697 [astro-ph.CO].
- [55] L. Alabidi, K. Kohri, M. Sasaki, and Y. Sendouda, JCAP **1209**, 017 (2012), arXiv:1203.4663 [astro-ph.CO].
- [56] N. Orlofsky, A. Pierce, and J. D. Wells, Phys. Rev. D **95**, 063518 (2017), arXiv:1612.05279 [astro-ph.CO].
- [57] T. Nakama, J. Silk, and M. Kamionkowski, Phys. Rev. D **95**, 043511 (2017), arXiv:1612.06264 [astro-ph.CO].
- [58] K. Inomata, M. Kawasaki, K. Mukaida, Y. Tada, and T. T. Yanagida, Phys. Rev. D **95**, 123510 (2017), arXiv:1611.06130 [astro-ph.CO].
- [59] S.-L. Cheng, W. Lee, and K.-W. Ng, JCAP **1807**, 001 (2018), arXiv:1801.09050 [astro-ph.CO].
- [60] R. Easther, J. T. Giblin, Jr., and E. A. Lim, Phys. Rev. Lett. **99**, 221301 (2007), arXiv:astro-ph/0612294 [astro-ph].
- [61] S. Antusch, F. Cefala, and S. Orani, Phys. Rev. Lett. **118**, 011303 (2017), arXiv:1607.01314 [astro-ph.CO].
- [62] J. Liu, Z.-K. Guo, R.-G. Cai, and G. Shiu, Phys. Rev. Lett. **120**, 031301 (2018), arXiv:1707.09841 [astro-ph.CO].
- [63] A. Y. Kamenshchik, A. Tronconi, T. Vardanyan, and G. Venturi, Phys. Lett. B **791**, 201 (2019), arXiv:1812.02547 [gr-qc].
- [64] C. Chen and Y.-F. Cai, JCAP **1910**, 068 (2019), arXiv:1908.03942 [astro-ph.CO].
- [65] S. S. Mishra and V. Sahni, (2019), arXiv:1911.00057 [gr-qc].
- [66] C. Fu, P. Wu, and H. Yu, Phys. Rev. D **100**, 063532 (2019), arXiv:1907.05042 [astro-ph.CO].
- [67] C. Fu, P. Wu, and H. Yu, (2019), arXiv:1912.05927 [astro-ph.CO].
- [68] J. Liu, Z.-K. Guo, and R.-G. Cai, (2019), arXiv:1908.02662 [astro-ph.CO].
- [69] R.-G. Cai, Z.-K. Guo, J. Liu, L. Liu, and X.-Y. Yang, (2019), arXiv:1912.10437 [astro-ph.CO].
- [70] V. De Luca, V. Desjacques, G. Franciolini, and A. Riotto, JCAP **1909**, 059 (2019), arXiv:1905.13459 [astro-ph.CO].
- [71] S. A. Vallejo-Pena and A. E. Romano, (2019), arXiv:1911.03327 [gr-qc].
- [72] M. Sasaki, T. Suyama, T. Tanaka, and S. Yokoyama, Class. Quant. Grav. **35**, 063001 (2018), arXiv:1801.05235 [astro-ph.CO].
- [73] S. Passaglia, W. Hu, and H. Motohashi, Phys. Rev. D **99**, 043536 (2019), arXiv:1812.08243 [astro-ph.CO].
- [74] N. Bartolo, V. De Luca, G. Franciolini, A. Lewis, M. Peloso, and A. Riotto, Phys. Rev. Lett. **122**, 211301 (2019), arXiv:1810.12218 [astro-ph.CO].
- [75] R.-G. Cai, S. Pi, and M. Sasaki, Phys. Rev. Lett. **122**, 201101 (2019), arXiv:1810.11000 [astro-ph.CO].
- [76] C. Armendariz-Picon, T. Damour, and V. F. Mukhanov, Phys. Lett. B **458**, 209 (1999), arXiv:hep-th/9904075 [hep-th].
- [77] J. Garriga and V. F. Mukhanov, Phys. Lett. B **458**, 219 (1999), arXiv:hep-th/9904176 [hep-th].
- [78] T. Kobayashi, M. Yamaguchi, and J. Yokoyama, Phys. Rev. Lett. **105**, 231302 (2010), arXiv:1008.0603 [hep-th].
- [79] T. Kobayashi, M. Yamaguchi, and J. Yokoyama, Prog. Theor. Phys. **126**, 511 (2011), arXiv:1105.5723 [hep-th].
- [80] T. Kobayashi, M. Yamaguchi, and J. Yokoyama, Phys. Rev. D **83**, 103524 (2011), arXiv:1103.1740 [hep-th].
- [81] R. Herrera, N. Videla, and M. Olivares, Eur. Phys. J. C **78**, 934 (2018), arXiv:1806.04232 [gr-qc].
- [82] N. C. Tsamis and R. P. Woodard, Phys. Rev. D **69**, 084005 (2004), arXiv:astro-ph/0307463 [astro-ph].
- [83] W. H. Kinney, Phys. Rev. D **72**, 023515 (2005), arXiv:gr-qc/0503017 [gr-qc].
- [84] Z. Yi and Y. Gong, JCAP **1803**, 052 (2018), arXiv:1712.07478 [gr-qc].
- [85] K. Inomata and T. Nakama, Phys. Rev. D **99**, 043511 (2019), arXiv:1812.00674 [astro-ph.CO].
- [86] K. Inomata, M. Kawasaki, and Y. Tada, Phys. Rev. D **94**, 043527 (2016), arXiv:1605.04646 [astro-ph.CO].
- [87] D. J. Fixsen, E. S. Cheng, J. M. Gales, J. C. Mather, R. A. Shafer, and E. L. Wright, Astrophys. J. **473**, 576 (1996), arXiv:astro-ph/9605054 [astro-ph].
- [88] B. J. Carr, Astrophys. J. **201**, 1 (1975).
- [89] S. Young, C. T. Byrnes, and M. Sasaki, JCAP **1407**, 045 (2014), arXiv:1405.7023 [gr-qc].
- [90] O. Özsoy, S. Parameswaran, G. Tasinato, and I. Zavala, JCAP **1807**, 005 (2018), arXiv:1803.07626 [hep-th].
- [91] Y. Tada and S. Yokoyama, Phys. Rev. D **100**, 023537 (2019), arXiv:1904.10298 [astro-ph.CO].
- [92] N. Aghanim *et al.* (Planck), (2018), arXiv:1807.06209 [astro-ph.CO].
- [93] I. Musco and J. C. Miller, Class. Quant. Grav. **30**, 145009 (2013), arXiv:1201.2379 [gr-qc].
- [94] T. Harada, C.-M. Yoo, and K. Kohri, Phys. Rev. D **88**, 084051 (2013), [Erratum: Phys. Rev. D **89**, no. 2, 029903 (2014)], arXiv:1309.4201 [astro-ph.CO].
- [95] T. Nakamura, M. Sasaki, T. Tanaka, and K. S. Thorne, Astrophys. J. **487**, L139 (1997), arXiv:astro-ph/9708060 [astro-ph].
- [96] K. Kohri and T. Terada, Phys. Rev. D **97**, 123532 (2018), arXiv:1804.08577 [gr-qc].
- [97] Y. Lu, Y. Gong, Z. Yi, and F. Zhang, JCAP **1912**, 031 (2019), arXiv:1907.11896 [gr-qc].
- [98] R. D. Ferdman *et al.*, *Gravitational waves. Proceedings, 8th Edoardo Amaldi Conference, Amaldi 8, New York, USA, June 22-26, 2009*, Class. Quant. Grav. **27**, 084014 (2010), arXiv:1003.3405 [astro-ph.HE].
- [99] G. Hobbs *et al.*, *Gravitational waves. Proceedings, 8th Edoardo Amaldi Conference, Amaldi 8, New York, USA, June 22-26, 2009*, Class. Quant. Grav. **27**, 084013 (2010), arXiv:0911.5206 [astro-ph.SR].
- [100] M. A. McLaughlin, Class. Quant. Grav. **30**, 224008 (2013), arXiv:1310.0758 [astro-ph.IM].
- [101] G. Hobbs, Class. Quant. Grav. **30**, 224007 (2013), arXiv:1307.2629 [astro-ph.IM].
- [102] C. J. Moore, R. H. Cole, and C. P. L. Berry, Class. Quant. Grav. **32**, 015014 (2015), arXiv:1408.0740 [gr-qc].
- [103] G. M. Harry (LIGO Scientific), Class. Quant. Grav. **27**, 084006 (2010).
- [104] J. Aasi *et al.* (LIGO Scientific), Class. Quant. Grav. **32**, 074001 (2015), arXiv:1411.4547 [gr-qc].
- [105] K. Danzmann, Class. Quant. Grav. **14**, 1399 (1997).
- [106] P. Amaro-Seoane *et al.* (LISA), (2017), arXiv:1702.00786 [astro-ph.IM].
- [107] W.-R. Hu and Y.-L. Wu, Natl. Sci. Rev. **4**, 685 (2017).
- [108] J. Luo *et al.* (TianQin), Class. Quant. Grav. **33**, 035010

- (2016), arXiv:1512.02076 [astro-ph.IM].
- [109] E. Thrane and J. D. Romano, Phys. Rev. D **88**, 124032 (2013), arXiv:1310.5300 [astro-ph.IM].
- [110] C. Yuan, Z.-C. Chen, and Q.-G. Huang, (2019), arXiv:1910.09099 [astro-ph.CO].
- [111] S. Kuroyanagi, T. Chiba, and T. Takahashi, JCAP **1811**, 038 (2018), arXiv:1807.00786 [astro-ph.CO].